ELSEVIER

Polymer 40 (1998) 207–218

polymer

Spread films of polymethyl methacrylate on aqueous solutions of polyethylene oxide

S.K. Peace[a], R.W. Richards[a,*], F.T. Kiff[a], J.R.P. Webster[b], N. Williams[c]

[a]*Interdisciplinary Research Centre in Polymer Science and Technology, University of Durham, Durham DH1 3LE, UK*
[b]*ISIS Science Division, Rutherford Appleton Laboratory, Chilton, Didcot, Oxfordshire OX11 0QX, UK*
[c]*ICI Paints Ltd., Wexham Road, Slough, Berkshire SL2 5DS, UK*

Revised 13 March 1998

Abstract

Polymethyl methacrylate has been spread on a 0.1% (w/v) aqueous solution of polyethylene oxide. The near surface organisation of both polymers and the water has been determined using neutron reflectometry. Both deuterio and hydrogenous forms of both polymers were available and the reflectivity data at the lower concentration of polymethyl methacrylate investigated (1.0 mg m^{-2}) could be interpreted using the kinematic approximation. At this lower concentration both polymethyl methacrylate and polyethylene oxide regions require a two-layer model to fit the reflectivity data. The thickness of the denser methacrylate near the water surface is 22 Å, the less dense layer further into the air phase has a thickness of 28 Å but a concentration one-tenth of the dense layer. At the higher concentration of polymethyl methacrylate (3.0 mg m^{-2}) the near surface water layer becomes very diffuse and broad, and the full kinematic approximation could only be used for the polymethyl methacrylate reflectivity data. A two-layer model again gave the best fit to the data with thicknesses not much greater than those at the lower surface concentration, however the total concentration of polymethyl methacrylate was now much lower than that dispensed, suggesting the existence of a third layer which was so low in concentration of polymer that it contributed but little to the reflectivity. Using the optical matrix analysis method, the near surface water layer was modelled as a single very diffuse layer to which the majority of the polyethylene oxide was confined. The thickness of this uniform layer of polyethylene oxide was 37 Å, almost double the thickness of the layer at the lower polymethyl methacrylate surface concentration. No polyethylene oxide was desorbed from the interface, the surface concentration was identical for both surface concentrations of polymethyl methacrylate and of the same value as that obtained in the absence of a spread polymethyl methacrylate film.

Keywords: Spread-film; Organisation; Reflectometry

1. Introduction

An understanding of the organisation of polymers at fluid interfaces is relevant to a number of areas. Polymers at liquid–liquid interfaces play a role in emulsion stability, liquid–liquid extraction and the organisation at such interfaces is evidently of importance in wet-bath spinning of fibres (e.g. defining skin–core morphology differences). At air–liquid interfaces the molecular organisation may determine the nature of resultant Langmuir–Blodgett films and thus may be manipulated to control capillary wave properties. In both situations, polymers at such interfaces have a pseudo two-dimensional structure and the properties of such confined polymer molecules are of intrinsic interest.

The simplest interface is the air–liquid interface although the resultant arrangement may be complex if the polymer has an amphiphilic nature and the liquid phase is water. In some cases the arrangement of the polymer at the interface may be relatively simple. This was the case for spread films of polymethyl methacrylate [1–3], but detailed analysis of a higher methacrylate [4] revealed an unexpected partial immersion of the hydrophobic substituent in the aqueous subphase. For a linear block copolymer of polymethyl methacrylate and polyethylene oxide, evidence for interfacial demixing as the surface concentration increased was obtained [5]. When a graft copolymer of the same two constituents was investigated, it was found that the polyethylene oxide grafts were immersed in the aqueous subphase from the outset, increases in the surface concentration were accompanied by an increased depth of penetration into the subphase by the grafts [6]. This was suggestive of the formation of a brush-like layer but definitive evidence for this was not obtained. Others have reported

* Corresponding author.

0032-3861/98/$ - see front matter
PII: S0032-3861(98)00234-1

the formation of brushes of polyethylene oxide when a linear diblock copolymer was spread at the surface [7].

It is well known that aqueous solutions of polyethylene oxide have an excess surface layer at equilibrium, and both the nature and composition of this surface layer have been quantified by neutron reflectometry [8]. In view of the spectrum of organisational behaviour of block and graft copolymers of polymethyl methacrylate and polyethylene oxide (and the respective homopolymers) when spread at the air–water interface, it is pertinent to enquire into the organisation of these two homopolymers in the presence of each other. We report here on the application of neutron reflectometry to spread layers of polymethyl methacrylate on a 0.1% (w/v) aqueous solution of polyethylene oxide. The thickness of the polymer-rich regions, and their composition, have been obtained at two surface concentrations of polymethyl methacrylate. Simple models are incapable of reproducing the experimental data and the organisation of the two polymer layers and the associated near surface water layer is complex. The description obtained should be contrasted with that of diblock and graft copolymers of the same two species that apparently have a much simpler organisation at the air–water interface.

2. Theoretical background

Exact reconstruction of the neutron reflectivity profiles (i.e. the ratio of the reflected intensity to incident beam intensity as a function of scattering vector Q, where $Q = 4\pi/\lambda (\sin\theta)$ for a neutron beam of wavelength λ and grazing incidence angle θ), obtained when a beam of neutrons is reflected from an interface can be obtained using the so-called optical matrix method and a knowledge of the coherent neutron scattering length density in each of the relevant surface regions. This method has been described many times before and we do not elaborate further on it here [9,10]. For air–water interfaces where the reflectivity is intrinsically small, it is sometimes possible to obtain as detailed an insight as with the optical matrix method but with less uncertainty as to the uniqueness of the description by using the kinematic approximation. This was originally outlined by Als-Nielsen [11], but has been developed to a high degree and applied to surfactants by Thomas [10]. There have been limited applications of this method to polymers at air–water interfaces [1,2,4–6]. Since much use of this approach will be subsequently made here, we set out the basic equations to be used. Detailed discussions of the kinematic approximation and its development have been provided elsewhere [10].

For the reflection of a neutron beam from the surface region of a liquid which contains polymethyl methacrylate, polyethylene oxide and water (signified by subscripts m, e, w respectively), the reflectivity in the kinematic approximation is given by;

$$R(Q) = \frac{16\pi^2}{Q^2}\left[b_m^2 h_{mm}(Q) + b_e^2 h_{ee}(Q) + b_w^2 h_{ww}(Q) + 2b_m b_e h_{me}(Q) + 2b_m b_w h_{mw}(Q) + 2b_e b_w h_{ew}(Q)\right] \quad (1)$$

where $h_{ii}(Q)$ represents self-partial structure factors and $h_{ij}(Q)$ the cross-partial structure factors and b_i are coherent scattering lengths for the m, e, and w constituent units. Self-partial structure factors contain information on the composition and thickness of the region occupied by species i and they are the square of the one-dimensional Fourier transform of the number density distribution of species i normal to the plane on which the beam is incident.

$$h_{ii}(Q) = |n_i(Q)|^2 \quad (2)$$

Expressions for $h_{ii}(Q)$ that can be used to interpret partial structure factors can be developed for relatively simple models of the distribution, e.g. a uniform layer, and are given later when we discuss our results.

The cross-partial structure factors, $h_{ij}(Q)$, have information within them about the separation between the i and j regions at the surface and $h_{ij}(Q) = \mathrm{Re}|n_i(Q)n_j(Q)|$. If the two regions have an even distribution (i.e. a symmetrical distribution of species i and j about their respective centres), and the centres of these two distributions are separated by a distance δ then

$$h_{ij}(Q) = \pm (h_{ii}(Q)h_{jj}(Q))^{1/2} \cos(Q\delta) \quad (3)$$

Even distributions are generally applicable to polymer layers at an interface. When one distribution is even and one odd then

$$h_{ij}(Q) = \pm (h_{ii}(Q)h_{jj}(Q))^{1/2} \sin(Q\delta) \quad (4)$$

The distribution of water is represented by an odd function since the near surface region of the aqueous phase increases in density over a finite length range to that of the bulk and this bulk density extends over an infinite distance as far as neutron reflectivity is concerned.

Since there are six partial structure factors in Eq. (1), obtaining each requires reflectivity data to be collected for six different contrasts, i.e. different values of b_i. To facilitate this necessary range of contrasts the aqueous phases used are generally null reflecting water (a mixture of H_2O and D_2O with a scattering length density of zero) and D_2O. For D_2O subphases Crowley and co-workers [12,13] pointed out the necessity of correcting the reflectivity before it is used in Eq. (1) because of the failure of the kinematic approximation to describe the reflectivity accurately when its value becomes large, $>10^{-2}$ approximately. The six sets of reflectivity data expressed as in Eq. (1) are then solved simultaneously to provide the self- and cross-partial structure factors at each Q value used.

Table 1
Molecular weights and molecular weight distributions

Polymer	$\bar{M}_w/10^{-3}$	$\bar{M}_n/\bar{M}_n$
hPEO	89.6	1.06
dPEO	83.7	1.20
hPMMA	121.0	1.35
dPMMA	110.6	1.21

3. Experimental

Hydrogenous and deuterated isomers of polymethyl methacrylate (PMMA) and polyethylene oxide (PEO) were synthesised by anionic polymerisation under high vacuum. For the PMMA fluorenyl lithium was used as the initiator and polymerisation was carried out at 195 K in tetrahydrofuran. Degassed methanol was used to terminate the reaction and the polymer precipitated out in methanol and dried under vacuum at 313 K. PEO syntheses were also carried out in tetrahydrofuran at 340 K using diphenyl methyl potassium as initiator. The polymerisation was terminated by adding ethanoic acid and the polymer precipitated out in hexane before drying under vacuum. The molecular weights and molecular weight distributions obtained using SEC (chloroform solvent and polystyrene calibration) are given in Table 1. ^{1}H n.m.r. on the PMMA confirmed that these polymers were ~80% syndiotactic.

3.1. Surface pressure isotherms

A NIMA System 1400 Langmuir film balance was used to obtain the surface pressure isotherms. This film balance has two barriers that close symmetrically about the position of the Wilhelmy plate used as the surface pressure sensor. This symmetrical closing means that forces on either side of the Wilhelmy plate are balanced, and it is not displaced from the equilibrium vertical position as the surface spread polymer film becomes stiff at high values of the surface concentration, Γ_s. To determine the surface pressure isotherm, the trough was filled with a 0.1% (w/v) solution of PEO in high purity water (Elgastat, UHQ). The surface of the solution was swept and aspirated to remove any adventitious surface contamination and then left for 10 min to attain the equilibrium surface excess concentration of PEO. A spread film of PMMA was then placed on the surface of the solution by depositing a small volume (typically 30 μl) of a 0.1% (w/v) solution of PMMA in chloroform on to the surface. The chloroform was allowed to evaporate for 15 min before the barriers were activated to reduce the initial area of 900 cm^2. The barrier speed was set so that the area decreased by 30 cm^2 min^{-1}. During this surface area reduction, the surface pressure was continuously recorded.

3.2. Neutron reflectometry

Neutron reflectivity data were obtained using the CRISP and SURF reflectometers at the UK pulsed neutron source ISIS at the Rutherford Appleton Laboratory. Two incident angles of the neutron beam on the liquid surface were used, 0.8 and 1.5°, the Q range covered was thus 0.025–0.65 Å^{-1}. The beam was incident on the liquid in a Langmuir trough placed on an anti-vibration plinth, spread films on PEO solution were prepared using a variety of combinations of deuterated and hydrogenous polymer with D_2O and null reflecting water (NRW). After spreading each film and compressing to the required surface concentration, a time of 40 min was allowed before commencing data collection. Prior experiments had shown that this time was required to allow complete relaxation of the spread film with a PMMA surface concentration of 3.0 mg m^{-2} and for the equilibrium surface pressure to be obtained. Although no relaxation was observed for the lower surface concentrations investigated here, this 40 min wait period was used for all spread films.

The combinations of polymer and subphase used were hPMMA/hPEO/D_2O, dPMMA/hPEO/D_2O, dPMMA/hPEO/NRW, hPMMA/dPEO/D_2O, dPMMA/dPEO/NRW and hPMMA/dPEO/NRW, and two surface concentrations of PMMA were explored, 1 and 3 mg m^{-2}. As well as the reflectivity data for the combinations listed above being obtained, reflectivity data for PMMA spread on water at a surface concentration of 3.0 mg m^{-2} and the solution of PEO (0.1%, w/v) were also obtained to establish the behaviour of each polymer in the absence of the other. All reflectivity data were normalised to incident neutron beam total flux and placed on an absolute basis using the reflectivity from D_2O as the calibrant. For the evaluation of partial structure factors it is important that the incoherent background signal is subtracted. In common with accepted practice the background was estimated as the average reflectivity calculated over the Q range 0.45–0.61 Å^{-1}. This method of estimating the background has been demonstrated to give the same result as obtaining the background from a separate measurement of the off-specular reflected signal.

4. Results

4.1. Surface pressure isotherm

The surface tension of the 0.1% PEO solution was found to be 63.6 ± 0.2 mN m^{-1} which is in agreement with data reported earlier by Lu et al. [8]. In common with Lu et al. we observed no long 'induction' times before a constant value of the surface tension was obtained. The equilibrium value was rapidly obtained and was stable thereafter. Fig. 1 shows the surface pressure isotherms recorded at 298 K for PMMA spread on water and PMMA spread on the 0.1% (w/v) PEO solution. There are clear differences in these two isotherms, when spread on the PEO solution the surface pressure increases gradually with no evidence for the abrupt increase

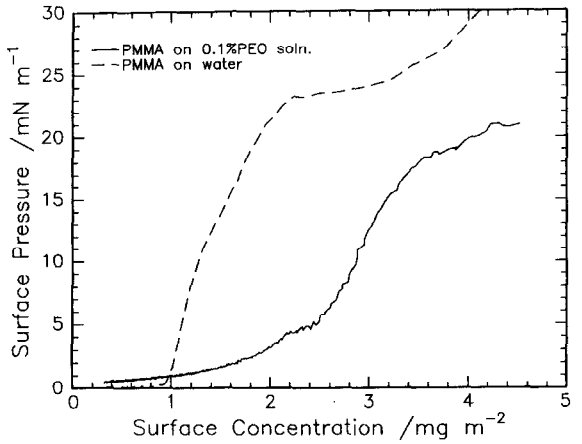

Fig. 1. Surface pressure isotherms at 298 K for polymethyl methacrylate on pure water and spread on a 0.1% (w/v) solution of polyethylene oxide in water.

observed when PMMA is spread on pure water [3,14–16]. The surface pressures recorded for the PMMA spread on PEO solution were generally much smaller than those recorded for PMMA on pure water. The increase in surface pressure from the outset suggests that the PMMA forms a continuous film on the PEO solution. The lower values of surface pressure recorded for the PMMA spread on 0.1% PEO solution, compared to that for the equivalent surface concentration on pure water, are symptomatic of desorption, i.e. either or both of the polymers (spread PMMA or adsorbed PEO) has a reduced contact with the surface. Generally, this implies there are a greater number of loops in the loop, train, tail structure that is used to describe polymers adsorbed at a surface [17]. Conclusions about the organisation of the two polymers at the interface can be obtained from a consideration of the neutron reflectometry data.

4.2. Neutron reflectometry

4.2.1. PMMA on PEO solution

Fig. 2(a) shows the reflectivity data for PMMA at a surface concentration of 1 mg m^{-2} spread on a solution of 0.1% (w/v) PEO in NRW. The reflectivities of each of the polymer combinations are in the order expected, i.e. largest

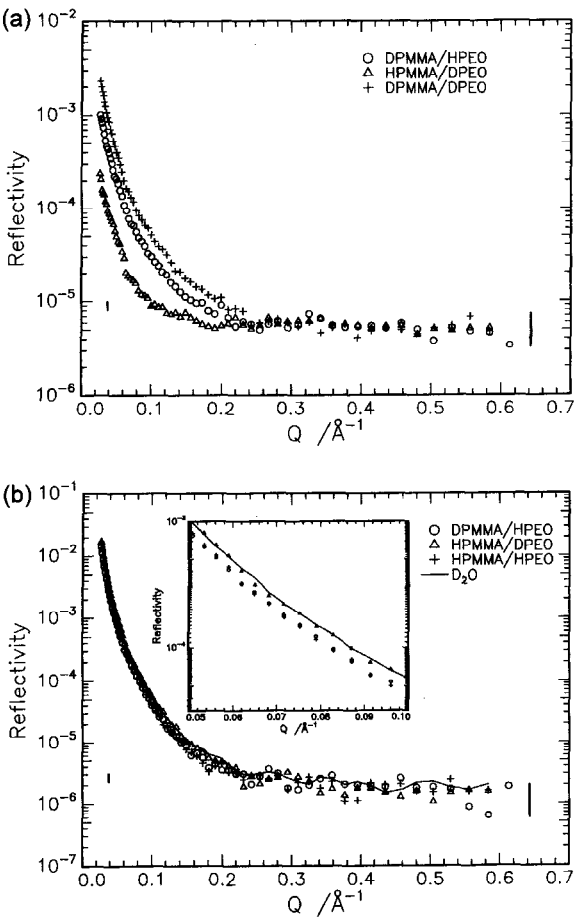

Fig. 2. Neutron reflectivity profiles (before background subtraction) when Γ_s of PMMA is 1 mg m^{-2} for the various isotopic combinations when (a) null reflecting water forms the subphase and (b) D_2O forms the subphase. The errors associated with the data in the extremes of the Q range are indicated by the vertical solid lines.

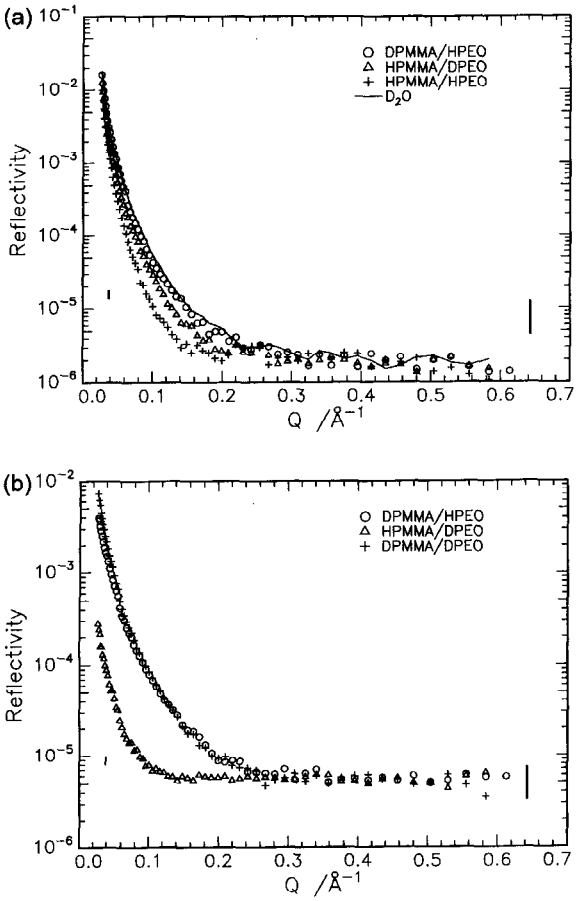

Fig. 3. Neutron reflectivity profiles for PMMA with Γ_s of 3 mg m^{-2} (a) D_2O as subphase and (b) null reflecting water as subphase. The inset shows the data at higher resolution and over a smaller Q range to show that differences between each of the reflectivity profiles exist. The errors associated with the data in the extremes of the Q range are indicated by the vertical solid lines.

reflectivity from the system containing the most deuterium. Note the shape of the reflectivity curves is the same for all, suggesting that the dimensions of the PMMA-rich and PEO-rich regions are similar. The fall in reflectivity on going from dPMMA/hPEO/NRW to hPMMA/dPEO/NRW is much greater than that from dPMMA/dPEO/NRW to dPMMA/hPEO/NRW. Clearly the dPMMA is the major source of the reflectivity, and it appears that the concentration of methacrylate units in the methacrylate rich region is high. Conversely, the PEO-rich region appears dilute which is qualitatively reasonable given that it is dissolved in the subphase. Neutron reflectometry profiles obtained when D_2O is used as the solvent for the PEO are shown in Fig. 2(b). All are rather similar to the reflectivity of pure D_2O, although the small reduction in reflectivity is most marked when both polymers are hydrogenous as expected. This depression in reflectivity relative to that of pure D_2O is most marked when the surface concentration is 3 mg m^{-2} (Fig. 3(a)). Note now that the shape of each reflectivity profile is suggesting that the natures of the PMMA-rich, PEO-rich and near surface water layers have different thickness. This view is confirmed for the two polymers when the reflectivity profiles on NRW are inspected (Fig. 3(b)). The reflectivity of the hPMMA/dPEO/NRW combination is much less than those systems where dPMMA is present because the dPEO is diluted by the subphase. The noteworthy feature is that the reflectivity curve for the hPMMA/dPEO/NRW combination is much steeper than the other two. This suggests that the dPEO-rich region is thicker than the dPMMA-rich region. What is also noteworthy is that the shapes of the neutron reflectivity profiles at $\Gamma_s = 3.0$ mg m^{-2} are very different to those for $\Gamma_s = 1.0$ mg m^{-2} and thus the near surface organisations are different from each other for these two surface concentrations of PMMA.

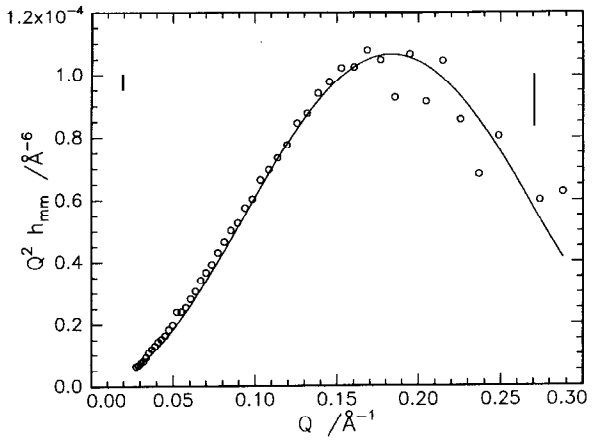

Fig. 4. Self-partial structure factor multiplied by Q^2 for PMMA at Γ_s = 3 mg m^{-2}. Solid line is a fit of a Gaussian distribution model. Errors are indicated by the vertical lines at the extremes of the Q range.

4.3. Individual homopolymers

4.3.1. PMMA spread on water at 3.0 mg m^{-2}

In our earlier work [1,3] on PMMA spread films on water the organisation at a surface concentration of 1 mg m^{-2} was obtained from neutron reflectometry data. However, a surface concentration of 3 mg m^{-2} was not explored at that time, consequently it is important that we know the organisation of the PMMA film at this concentration so that any changes when it is spread on 0.1% PEO solution become evident. Fig. 4 shows the self-partial structure factor (multiplied by Q^2) for the PMMA spread film at a surface concentration of 3 mg m^{-2} on pure water obtained by solution of simultaneous equations for the reflectivity as discussed earlier. Subtraction of background contributions to the reflectivity limits the maximum value of Q accessible to circa 0.25 Å^{-1}, and in this region both a uniform layer model and a Gaussian distribution of PMMA segments fit the data equally well and are *indistinguishable from each other*. Given the Gaussian nature of a polymer molecule we expect that the model based on a Gaussian distribution to be more appropriate. The number density of polymer segments is given by

$$n_p(z) = n_{pl} \exp(-4z^2/\sigma^2) \quad (5)$$

Where z is the distance from the mid point of the distribution where the number density is n_{pl} and σ is identified with the width of the distribution. From the Fourier transform of this distribution, the partial structure factor obtained is

$$Q^2 h_{pp}(Q) = \frac{n_{pl}^2 \pi \sigma^2 Q^2}{4} \exp(-Q^2\sigma^2/8) \quad (6)$$

The solid line in Fig. 4 is a non-linear least-squares fit of Eq. (6) to the data with n_{pl} and σ as the adjustable variables. The values obtained were $n_{pl} = (0.70 \pm 0.03) \times 10^{-2}$ Å^{-3} and $\sigma = 10 \pm 0.2$ Å; from these values the surface concentration can be calculated (Γ^c) using Eq. (7) where m

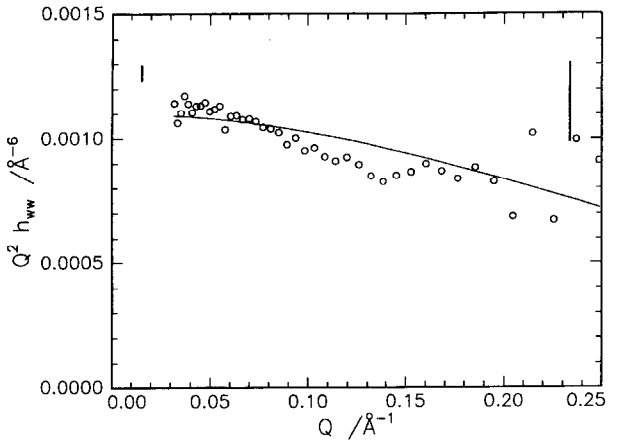

Fig. 5. Self-partial structure factor (multiplied by Q^2) for the near surface water layer at the same PMMA, surface concentration as for Fig. 4. Solid line is the fit of a tan h distribution of water molecules in the near surface region. Errors are indicated by the vertical lines.

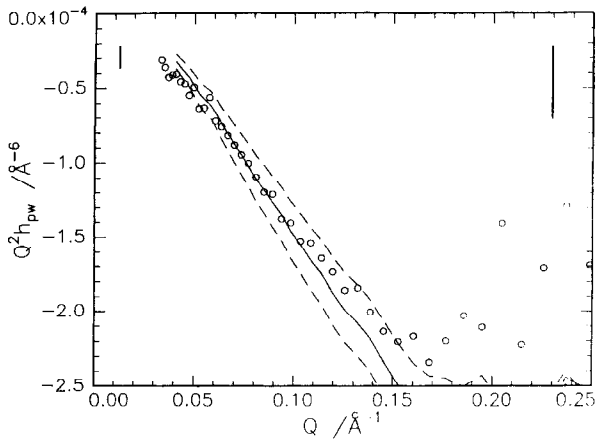

Fig. 6. Cross-partial structure factor between water and PMMA (Γ_s = 3 mg m^{-2}) compared with predictions from Eq. (4) with different values of δ. Solid line corresponds to a PMMA near-surface water region separation of 6.5 Å, dashed lines are ± 1 Å. Errors are indicated by the vertical lines at the Q range extremes.

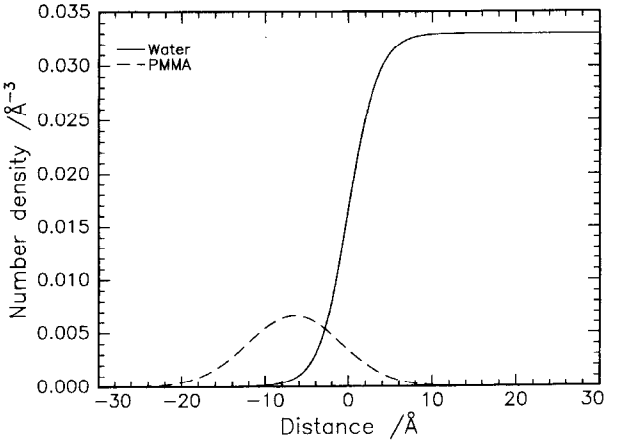

Fig. 7. Number density distribution of PMMA and near surface water layers for Γ_s = 3 mg m^{-2}.

(g mol^{-1}) is the molecular weight of the monomer unit and compared with the dispensed amount

$$\Gamma^c = \frac{\sigma n_{pl}\sqrt{\pi}m}{2N_A} \times 10^{23} \text{ mg m}^{-2} \quad (7)$$

The calculated surface concentration of PMMA is 1.9 ± 0.1 mg m^{-2} as compared to 3 mg m^{-2} dispensed on to the surface; we comment on this disparity later. We re-emphasise here that the fit of a uniform layer model to these data is equally as good and an identical value of the surface concentration is obtained from the parameters of this uniform layer model.

Fig. 5 shows the self-partial structure factor for the near surface water layer and the line through the data is a fit of the partial structure factor for a distribution of water molecules described by a hyperbolic tangent model

$$n_w(z) = n_{w0}(0.5 + 0.5 \tan h\,(z/\zeta)) \quad (8)$$

Where ζ is often called the width of the diffuse region. This function produces a partial structure factor given by

$$Q^2 h_{ww}(Q) = n_{w0}^2(\zeta\pi Q/2)^2 \text{ cosec } h^2(\zeta\pi Q/2) \quad (9)$$

where n_{w0} is the number density of water molecules an infinite distance from the surface, i.e. the bulk number density which for D_2O is 3.3 × 10^{-2} Å^{-3}. The best fit to the data is provided by a width ζ of 3.5 ± 0.1 Å. Fig. 6 shows the cross-partial structure factor between PMMA and the near surface water layer. Using the parameters obtained for the polymer and water self-partial structure factors, the product $(h_{pp}(Q)h_{ww}(Q))^{1/2}$ has been generated and multiplied by sin($Q\delta$) (see Eq. (4)) using different values of δ. The agreement with the experimental data is extremely sensitive to the value of δ as is apparent from Fig. 6; it appears that the centre-to-centre separation of the polymer and near surface water region distributions is 6.5 ± 0.5 Å. With all of these parameters available a number density distribution profile for the spread of PMMA on a water system can be constructed (Fig. 7), given the relatively hydrophobic nature of the PMMA, the centre of the PMMA distribution is placed on the air side of the subphase boundary. Note that some of the PMMA is immersed in the aqueous subphase but at least 60% is in the air phase.

The major concern regarding the analysis above is the poor agreement between the surface concentration of polymer actually placed on the surface and that calculated from the reflectivity. Earlier work on spread PMMA films [1,3] had demonstrated that, up to a surface concentration of circa 1.5 mg m^{-2}, there was perfect agreement between the value calculated from neutron reflectivity data and that actually dispensed. For greater values of Γ_s (and for atactic polymer, neutron reflectivity data were obtained for Γ_s values up to circa 5 mg m^{-2}), the neutron reflectivity calculated surface concentration was roughly constant at 1.9 ± 0.1 mg m^{-2}. Consequently, this appears to be a limiting concentration that can be accommodated on the surface in a layer dense enough to make a measurable contribution to the reflectivity. The polymer that is not contributing must loop away from the surface into the air-phase where the MMA segments become so 'dilute' they make negligible contribution to the reflectivity.

4.3.2. Solution of 0.1% (w/v) PEO

Although the nature of the surface excess layer in the PEO solution has been discussed earlier, we have re-investigated this aspect using the partial structure factor approach. We need to establish confidence that this method provides an equally accurate description as the exact optical matrix method used earlier. The same procedure as set out above was applied to the reflectivity data obtained for the 0.1% (w/v) solution of PEO in water. (Isotopic combinations used were dPEO/NRW, hPEO/D_2O, and dPEO/D_2O.) Gaussian and tan h distributions were again used to model the PEO and water distributions, the parameters obtained were; n_{pl} = (0.44 ± 0.01) × 10^{-2} Å^{-3}, σ = 18 ± 0.3 Å and ζ = 6.5 ± 0.3 Å. The values of n_{pl} and σ result in the

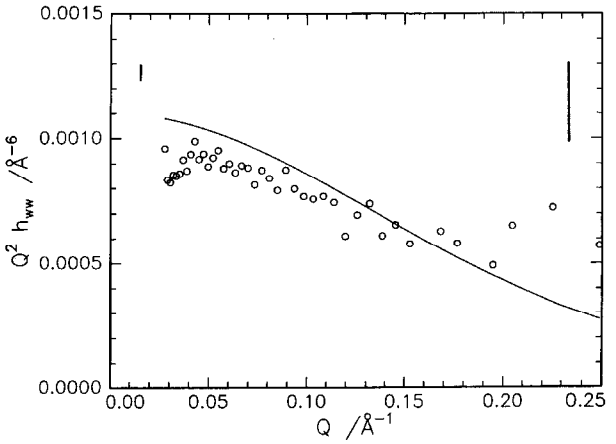

Fig. 8. Best fit of a tan h model for near surface water layer of a 0.1% PEO solution. The disparity between model and data at low Q is clearly evident.

surface concentration of PEO being 0.56 mg m^{-2}, this is in excellent agreement with the surface concentration obtained earlier [8], where the reflectometry data were analysed by exact optical matrix methods. A priori we anticipated that the centre of the PEO distribution and the water distribution would coincide, and thus the cross-partial structure factor would be zero. However, a small but finite cross-partial structure factor was obtained which was rather scattered at high Q and oddly did not display any tendency to approach zero as Q tends to zero. Attempts to reproduce this cross-partial structure factor using the two self-partial structure factor and finite values of the separation δ were not very successful, but suggest a separation of some 3 Å between the centres of the near surface water layer and the PEO layer. Disagreement at low Q between fit and data was the main problem, we believe this is due to the influence of PEO on the distribution of water because the water self-partial structure deviates quite significantly from the theoretical prediction as Q approaches zero (Fig. 8). This has been observed in other systems that contain PEO and, as yet, no convincing explanation has been offered. Therefore we can only say that the separation between PEO and water

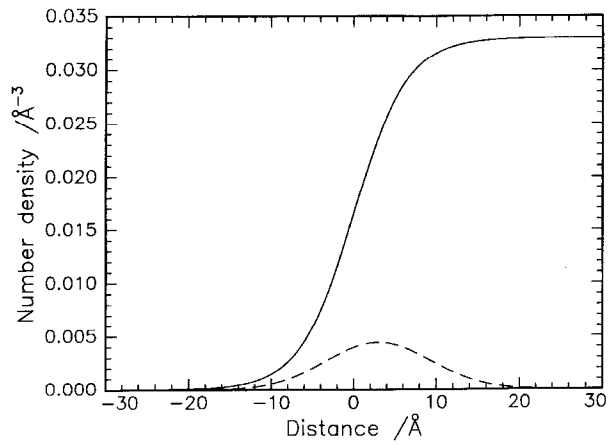

Fig. 9. Arrangement of PEO and water in the surface excess layer for a 0.1% (w/v) solution of PEO in water.

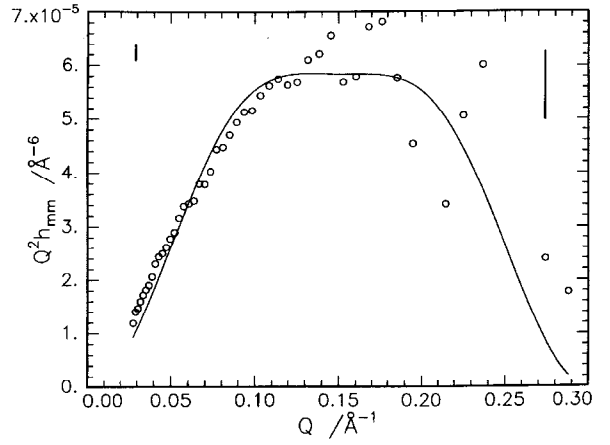

Fig. 10. Self-partial structure factor for PMMA with $\Gamma_s = 3$ mg m^{-2} on 0.1% (w/v) PEO solution. Solid line is best fit of two uniform layer model. Errors in the partial structure factor data are indicated by the vertical lines at the Q range extremes.

layers is small and of the order of 2–4 Å. Fig. 9 shows the distributions of PEO and water resulting from the parameters obtained, we have immersed the PEO in the water and moved the centre of the distribution 3 Å deeper into the subphase so that the PEO is totally immersed in the aqueous subphase.

4.4. Spread films of PMMA on 0.1% PEO solution

We analyse the partial-structure factor data for the two surface concentrations of PMMA on PEO solution separately, giving detailed description for the higher concentration data and restricting ourselves to pointing out differences when the lower concentration data were considered.

4.4.1. 3 mg m^{-2} PMMA

Fig. 10 shows the self-partial structure factor for the spread PMMA and neither a single uniform layer nor single Gaussian layer models fitted these data. A model consisting of two uniform layers reproduces the data well as shown by the solid line in Fig. 10. This model is described by the

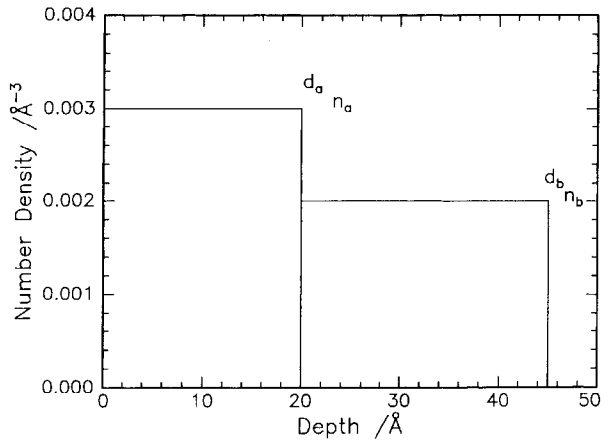

Fig. 11. Schematic of the distributions in a two uniform layer model of a surface film.

Table 2
Parameters of two-uniform layer model of PMMA

Γ_s (mg m^{-2})	d_a (Å)	n_a (10^{-2} Å^{-3})	d_b (Å)	n_b (10^{-3} Å^{-3})	Γ_s^c (mg m^{-2})
1.0	22 ± 1	0.25 ± 0.01	28 ± 2	0.24 ± 0.04	1.01 ± 0.2
3.0	26 ± 1	0.43 ± 0.01	32 ± 1	0.57 ± 0.04	2.1 ± 0.2

diagram in Fig. 11 and is specified as

$$n(z) = n_a \quad 0 < z < d_a$$

$$n(z) = n_b \quad d_a < z < d_b$$

The Fourier transform of this number density distribution is

$$n(Q) = \frac{n_b}{iQ}[\exp(-iQd_b) - \exp(-iQd_a)] + \frac{n_a}{iQ}[\exp(-Qd_a - 1] \tag{10}$$

and the resultant partial structure factor is:

$$h_{pp}(Q) = \frac{4\pi}{Q^2}\left[n_a(n_a - n_b)\sin^2\left(\frac{Qd_a}{2}\right) + n_a n_b \sin^2\left(\frac{Q(d_a + d_b)}{2}\right) - n_b(n_a - n_b)\sin^2\left(\frac{Qd_b}{2}\right)\right] \tag{11}$$

the values of the parameters obtained from the fit are given in Table 2.

The self-partial structure factors obtained from the rigorous kinematic approximation (i.e. Eq. (1)) for PEO in solution in the presence of the spread PMMA film were very slightly negative over the whole Q range. Negative values are not physically realistic because $h_{ii}(Q) = (n_i(Q))^2$. We attribute these negative values to two factors. Firstly, and most importantly, the reflectivity of the isotopic combinations where PEO was the only deuterated species present (and thus which determines $h_{ee}(Q)$) was significantly reduced from that in the absence of PMMA, and this reduction is particularly evident at the higher surface concentration of PMMA. Secondly, the small reflectivities result in the partial structure factor for the PEO being susceptible to random variation in all the reflectivities, because quantities of the same magnitude are being subtracted from each other and the partial structure factor values returned are small and negative over the Q range explored.

A second means by which the self-partial structure factor for PEO can be obtained is using the combination hPMMA/dPEO/NRW alone. The scattering length density of hPMMA can be approximated to zero and thus Eq. (1) becomes

$$R(Q) = \frac{16\pi^2}{Q^2} b_c^2 h_{ee}(Q) \tag{12}$$

consequently the self-partial structure factor for PEO can be approximated directly from the reflectivity data. Fig. 12 shows the self-partial structure factor for the PEO obtained in this way in the presence of PMMA; a weak, broad maximum is evident. Note that values of the partial structure factor are circa an order of magnitude smaller than those for PMMA in Fig. 10. A single-layer model (uniform or Gaussian distribution) fits this partial structure factor. The values of the parameters obtained from the fitting are given in Table 3.

The self-partial structure factor for the near surface water layer is shown in Fig. 13, evidently this is very different from that when each homopolymer is present alone (and for water self-partial structure factors obtained for other systems). The reflectivity measurements on the hPMMA/hPEO/D_2O system at a PMMA surface concentration of

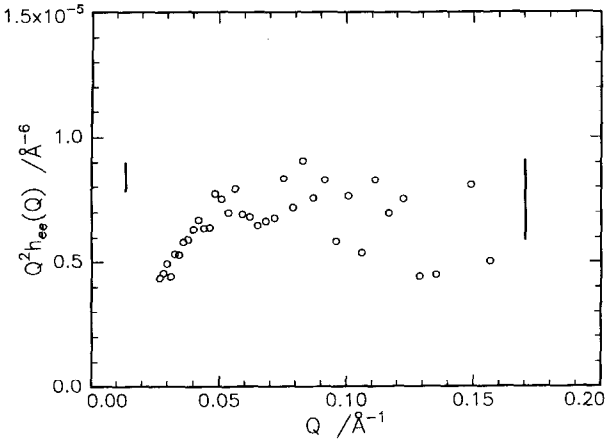

Fig. 12. Self-partial structure factors of dPEO obtained from the reflectivity data when the subphase was null reflecting water and the surface concentration of hPMMA 3.0 mg m^{-2}. Errors in the partial structure factor data are indicated by the vertical lines at the Q range extremes.

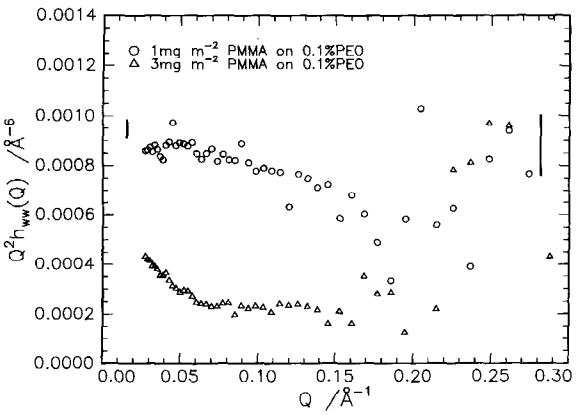

Fig. 13. Water self-partial structure factors obtained when Γ_s of PMMA spread on PEO solution is 1 and 3 mg m^{-2}. Errors in the partial structure factor data are indicated by the vertical lines at the Q range extremes.

Table 3
Parameters of uniform layer models for PEO in solution

Γ_s (mg m^{-2}) (PMMA)	d_a (Å)	n_a (10^{-2} Å^{-3})	d_b (Å)	n_b (10^{-3} Å^{-3})	Γ_s^{calc} (mg m^{-2}) (PEO)
1.0	22 ± 1	0.24 ± 0.01	37 ± 3	0.34 ± 0.01	0.46 ± 0.05
3.0[a]	37 ± 1	0.15 ± 0.01	—	—	0.44 ± 0.04

[a]A single uniform layer model was sufficient for this surface concentration of PMMA

3.0 mg m^{-2} were repeated some time later, but were identical with the first set. Consequently the water self-partial structure factor at a PMMA surface concentration of 3.0 mg m^{-2} shown in Fig. 13 is not an artefact.

Evidently conventional models of the near surface water layer are not applicable to these data. To obtain a description of the water layer we have resorted to fitting the reflectivity of the hPMMA/hPEO/D_2O combinations using the optical matrix method. We have used a single near surface water layer, the adjustable parameters of which are the scattering length density and the roughness at both air interface and the interface with the bulk of the D_2O subphase. The best fit obtained is shown in Fig. 14, and the parameters of the uniform layer fit are given in Table 3. Fig. 14 also shows the number density distribution that these numbers suggest for the water layer.

We have attempted to analyse the cross-partial structure factors to obtain separations between the distributions of PMMA, PEO and water molecules in the near surface region. For each combination we have used the actual partial structure factor data obtained in either Eq. (3) or Eq. (4) rather than generate data using partial structure factors from models of the distribution at the surface. Fig. 15 shows the cross-partial structure factor between PMMA and water, overlaid is that calculated using Eq. (4), and adjusting δ to give the best fit, the value obtained is given in Table 4. Table 4 also reports the separation between PMMA and PEO regions, the agreement between data and fit is shown in Fig. 16. Neither of these two fits is particularly good and this is because Eq. (3) and Eq. (4), to describe the cross-partial structure factors, are based on assumptions that are not strictly valid here, i.e. the polymer layers are uniform. Since we have demonstrated that the PMMA region consists of two layers, it is not surprising that complete agreement is not obtained. Using Eq. (4) is commensurate with ignoring the lower more diffuse layers for each polymer. Since the number density of polymer in these lower layers is circa an order of magnitude smaller than that in the upper layers this is probably not too serious an oversimplification. A major problem is the determination of the separation between the near surface water layer and the surface excess layer of PEO; the data and the best approximation using Eq. (4) are shown in Fig. 17. Although the shape of the data is recovered, the absolute value is not. In using Eq. (4), the partial structure factor for the PEO has been calculated from the hPMMA/dPEO/NRW data and Eq. (12), although this may introduce some error, the main source of this discrepancy is the fact that the water layer is so very diffuse and the simple product of partial structure factors fails as a model for the cross-partial structure factor.

4.4.2. 1.0 mg m^{-2} PMMA

At the lower surface concentration of PMMA a two-layer model was still required to fit the self-partial structure factor of the spread PMMA film, the parameters are reported in Table 2. A two-layer model was also needed to reproduce the self-partial structure factor of the PEO surface excess layer; values of the number density and thickness are reported in Table 3. Cross-partial structure factors between all the constituents of the near surface region were obtained

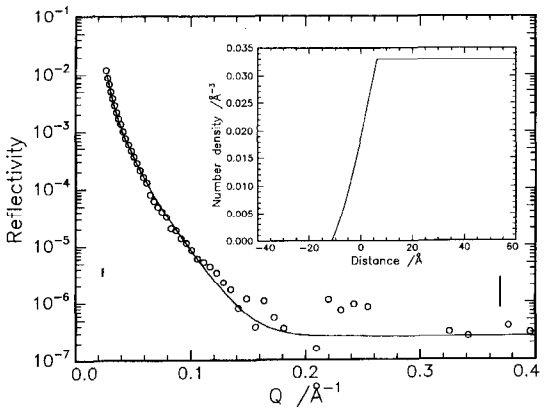

Fig. 14. Fit of a single-layer model with a diffuse interface for the near surface water layer to the reflectivity of hPMMA/hPEO/D_2O when Γ_s PMMA is 3.0 mg m^{-2}. Inset is the number density distribution implied by the fit.

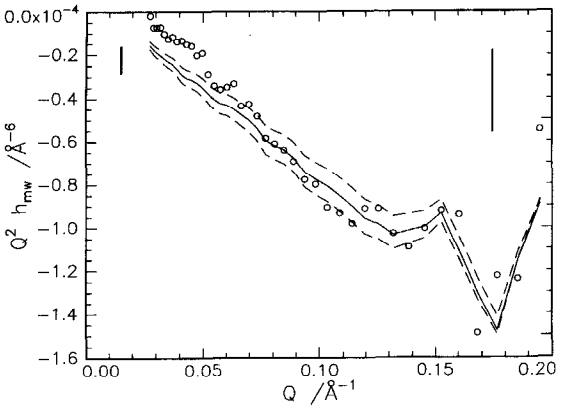

Fig. 15. Cross-partial structure factors between PMMA (Γ_s = 3.0 mg m^{-2}) and water compared with the predictions of Eq. (4) (solid line), the dashed lines are the cross-partial structure factors obtained using values of δ ± 1 Å. Errors in the partial structure factor data are indicated by the vertical lines at the Q range extremes.

Table 4
Separation between polymer and near surface water layers

PMMA Γ_s (mg m^{-2})	PMMA–water	δ (Å) PEO–water	PMMA–PEO
1	4 ± 1	0 ± 1	4 ± 1
3	8 ± 1	?	12 ± 1

in the same manner as described above, and for this lower surface concentration there was no uncertainty in obtaining the PEO–water separation because the water self-partial structure factor was of the form usually observed (see Fig. 13), i.e. not 'distorted' as observed when the PMMA concentration is 3.0 mg m^{-2}. All the values of the separations are given in Table 4. We draw attention to the surface concentrations of PEO in Table 3 obtained from the parameters of the partial structure factors. Both are identical and very close to the value obtained when there is no spread film of PMMA present. This is strong evidence for the accuracy of the models employed.

5. Discussion

At this point it is appropriate to attempt a summary of the detailed analysis of the reflectivity data before embarking on any discussion. For the two homopolymers alone (PMMA spread on water; the surface excess in PEO solution), the data concur either with that obtained by others or trends observed earlier and the same conclusions regarding their organisation at the air–water interface can be made. Even the inconsistency between spread surface concentration and calculated surface concentration for PMMA is reproduced.

When PMMA is spread at a surface concentration of 1 mg m^{-2} on a 0.1% (w/v) solution of PEO, neither polymer-rich region is describable by a single-layer model. In both cases we have had to use a double-layer model.

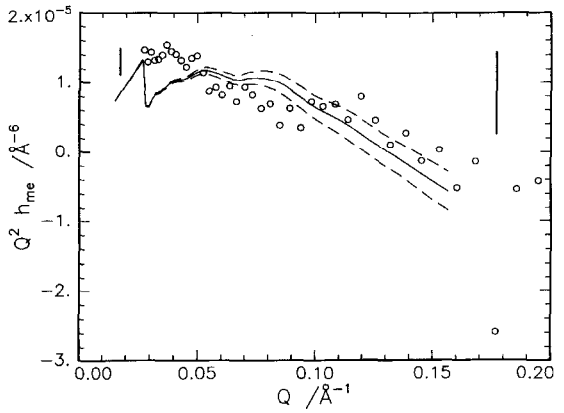

Fig. 16. Cross partial structure factor between PEO and PMMA for the same conditions as in Fig. 15. The dashed lines are the cross partial structure factors obtained using values of $\delta \pm 1$ Å. Errors in the partial structure factor data are indicated by the vertical lines at the Q range extremes.

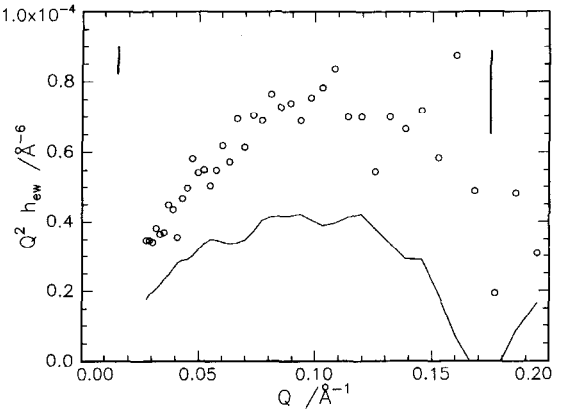

Fig. 17. Cross-partial structure factor between PEO and near surface water layer. The solid line is the closest obtained by using the self-partial structure factors and adjusting the value of δ in Eq. (4). Errors in the partial structure factor data are indicated by the vertical lines at the Q range extremes.

Although we have used double-uniform layer models we emphasise that we can equally well fit these data using double Gaussian distributions. An additional parameter is introduced in this latter model, the separation between the maxima of the Gaussians. The quality of the fits is not sensitive to the value of this separation and the improvement in the fit gained by using this double Gaussian distribution did not warrant the additional complexity, hence it was not pursued further. The surface concentration of PEO is not reduced by the presence of the PMMA spread layer, but the PEO-rich region becomes much more diffuse. Initially at low surface concentrations of PMMA some of the PEO forms a second (deeper) layer which is very dilute in PEO. At the higher PMMA surface concentration, 3 mg m^{-2}, the PEO surface excess region becomes a single very broad layer with a reduced number density of PEO compared to that in the absence of a spread PMMA film.

That the near surface water layer is made more diffuse as the PMMA surface concentration increases is unexpected, because the diffuse water layer, when PMMA is spread on pure water, essentially has the dimensions of the amplitude of capillary wave fluctuations [18]. At the lower PMMA surface concentration, the neutron reflectivity responds to all of the PMMA on the surface, because the surface concentration obtained agrees with that placed on the surface, notwithstanding the presence of the dilute second layer. Before we can sketch out the concentration profile of all species at the surface, we need to decide the order in which the layers follow each other. It is reasonable to place the more dilute PEO layer deeper into the subphase. However, for the PMMA the sequencing of the two layers is not so easily made because the disordering of the near surface water layer may be a source of some increased mixing of the water layer with the PMMA. We consider the scattering length density variation for the two possible arrangements of dPMMA on 0.1% hPEO in D_2O ignoring the presence of the PEO. One where the denser PMMA layer occupies the region closest to the water surface, and one

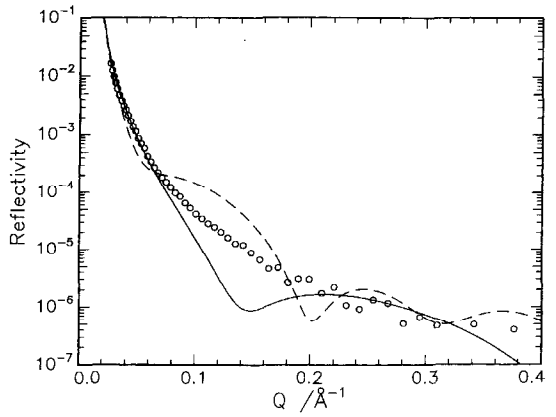

Fig. 18. Neutron reflectivity for $\Gamma_s = 3$ mg m^{-2} dPMMA on 0.1% (w/v) hPEO in D_2O compared (i.e. not a fit) to the reflectivity calculated for a two-layer model. The solid line has the denser PMMA layer nearer the water surface and the dashed line is for the case where the denser layer is uppermost (i.e. further away in the air phase).

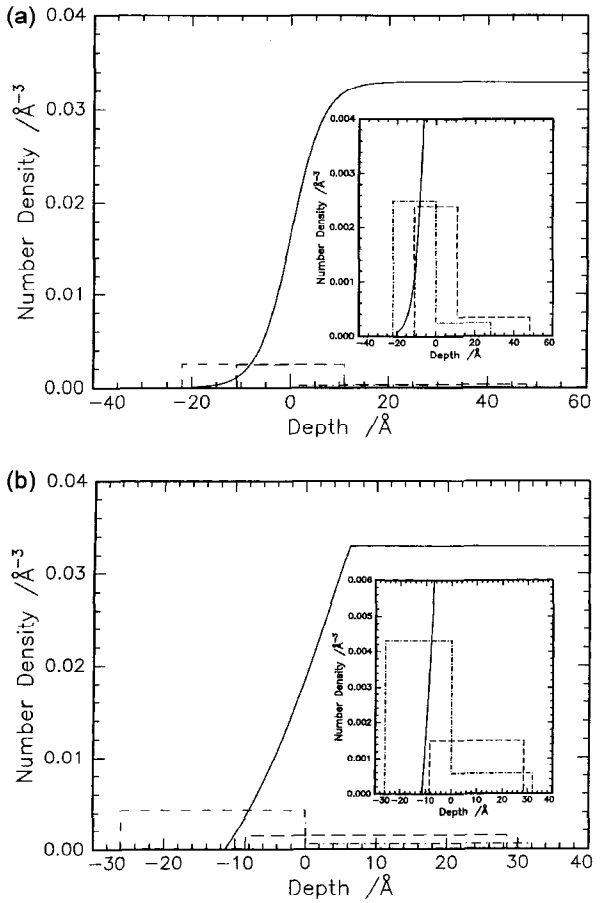

Fig. 19. Schematic sketch of the number density distribution for all components at the air–solution interface when PMMA is spread on an aqueous solution of 0.1% PEO. (a) PMMA surface concentration 1 mg m^{-2}; (b) PMMA surface concentration 3 mg m^{-2}. Insets show a more detailed sketch of the surface region. (———) Water; (– – –) PMMA; (– – –) PEO.

where it is further away from the water surface, i.e. more in the air phase. The reflectivities calculated from these two arrangements are compared with the experimental data in Fig. 18; exact agreement is not obtained because we have ignored the hPEO. However, the actual reflectivity is more akin to the simulation where the denser PMMA layer is nearer the water surface.

At the higher concentration of PMMA on the surface, the PMMA still seems to be mainly confined to two layers that have not increased their dimensions significantly. Although the number density of PMMA segments has increased in both layers, this is not in proportion to the greater amount deposited on the surface. Note that the increase in concentration of the dilute uppermost layer is (relatively) greater than that in the denser layer. Together with the underestimate of the total concentration of the PMMA at the surface, this seems to indicate that some of the PMMA is located in a third layer at greater distances from the water surface. The concentration of PMMA units in this third layer is so low that no effective contribution to the reflectivity is detected. Given that ca. one-third of the PMMA is located in the postulated third layer it must be quite thick to incorporate this polymer at low concentrations required to be ineffective in the reflectivity. The PEO layer in the presence of this higher PMMA surface concentration now occupies a broad, very diffuse region, but we point out that the surface concentration determined from both parameter sets is constant and little reduced from that obtained in the absence of PMMA on the surface. The major surprise here is the very disordered water layer which is now very diffuse and has a self-partial structure factor which cannot be reproduced by currently accepted models. Because of this we are unable to estimate the separation between the PEO-rich region and the near surface water layer. Presumably the diffuse water layer is intimately associated with the PEO and the centre of this distribution is coincident with that of the water. Fig. 19 is an attempt to sketch out the distributions of PMMA and PEO at the two surface concentrations of PMMA investigated. For the higher PMMA concentration we have overlaid the number density variation of the near surface water layer obtained from the fit to the reflectivity profile of hPMMA/hPEO/D_2O discussed earlier.

6. Conclusions

Using neutron reflectometry and making full use of the neutron contrasts accessible with deuterated polymers and aqueous subphase, we have demonstrated that the surface organisation for polymethyl methacrylate spread on a 0.1% solution of polyethylene oxide is considerably more complex than would have been anticipated from that of the individual homopolymers. At low surface concentrations of polymethyl methacrylate it is necessary to

use two layer models for both polymers to reproduce the observed partial structure factors obtained by a kinematic approximation analysis of the neutron reflectivity data. The polymethyl methacrylate is partially immersed and intermixed with the polyethylene oxide that is totally immersed in the aqueous phase.

At the highest surface concentration of polymethyl methacrylate investigated here, a two-layer model is still necessary to reproduce the partial structure factor, but there appears to be a third more dilute layer restricted entirely to the air phase. The polyethylene oxide layer has now become a single very broad layer but the total concentration of polyethylene oxide is not significantly reduced from that in the surface excess layer obtained in the absence of polymethyl methacrylate. The greatest influence is observed on the near surface water layer that now seems to be very diffuse and the partial structure factor which cannot be described by current popular models.

Acknowledgements

ICI Paints and EPSRC are thanked for the award of a CASE award to SKP. EPSRC and CCLRC are thanked for the support and provision of neutron beams and instrumentation at ISIS.

References

[1] Henderson JA, Richards RW, Penfold J, Thomas RK. Macromolecules 1993;26:65.
[2] Henderson JA, Richards RW, Penfold J, Thomas RK. Acta Polymerica 1993;44:184.
[3] Henderson JA, Richards RW, Penfold J, Shackleton C, Thomas RK. Polymer 1991;32:3284.
[4] Reynolds I, Richards RW, Webster JRP. Macromolecules 1995;28:7845.
[5] Richards RW, Rochford BR, Webster JRP. Faraday Discussions 1994;98:263.
[6] Peace SK, Richards RW, Williams N. Macromolecules, 1997, submitted.
[7] Bijsterbosch HD, de Haan VO, de Graaf AW, Mellema M, Leermakers FAM, Cohen-Stuart M, van Well AA. Langmuir 1995;11:4467.
[8] Lu JR, Su TJ, Thomas RK, Penfold J, Richards RW. Polymer 1996;37:109.
[9] Russell TP. Materials Science Reports 1990;5:171.
[10] Thomas RK. In: Richards RW, editor. Neutron reflection from polymer bearing surfaces. London: Ellis Horwood, 1995.
[11] Als-Nielsen J. Physica B + C 1984;126:145.
[12] Crowley TL, Lee EM, Simister EA, Thomas R, Penfold J, Rennie AR. Colloids and Surfaces 1990;52:85.
[13] Crowley TL, Lee EM, Simister EA, Thomas RK. Physica B 1991;174:143.
[14] Kawaguchi M. Prog Polym Sci 1993;18:341.
[15] Poupinet D, Vilanove R, Rondelez F. Macromolecules 1989;22:2491.
[16] Vilanove R, Rondelez F. Phys Rev Lett 1980;45:1502.
[17] Fleer GJ, Cohen-Stuart MA, Scheutjens JMHM, Cosgrove T, Vincent B. Polymers at interfaces. London: Chapman and Hall, 1993.
[18] Langevin D. In: Light scattering by liquid surfaces and complementary techniques, vol. 41. New York: Marcel Decker, 1992.